Ferrimagnetically ordered nanosized polyoxomolybdate-based cluster spheres†

Bogdan Botar,*[a] Paul Kögerler,*[b] Achim Müller,[c] Ricardo Garcia-Serres[d] and Craig L. Hill*[a]

Received (in Cambridge, UK) 31st August 2005, Accepted 11th October 2005
First published as an Advance Article on the web 20th October 2005
DOI: 10.1039/b512244a

The self-assembly of molybdate building units in the presence of Fe^{II} and V^{IV} produces the first mixed-spin heterometal keplerate-type clusters displaying ferrimagnetic interactions.

The rational design of nanosized molecule-based materials with the scope of carefully tuning their electronic[1a] and magnetic[1b] properties on the molecular scale is of considerable current interest. Giant polyoxomolybdate clusters, aside from interest in their unique structures and topologies,[2] are of special importance in this context as they can provide highly symmetric, rigid, nanometer-sized inorganic framework molecules that can be electronically and magnetically functionalized, by, for example, step-wise integration of heterometals. This versatility is exemplified by the family of doughnut-shaped, D_{3h}-symmetric $\{Mo_{57}M_6\}$-type cluster anions, in which a large range of heterometal cations M = Fe^{II}, Fe^{III}, V^{IV}, or Cu^{II} and mixtures thereof are embedded in a $\{Mo_{57}\}$ structure to form a trigonal spin prism,[3] for which antiferro-,[3a] ferri-,[3b] or ferromagnetic[3c] coupling is observed. Spherical keplerate cluster shells, based on twelve pentagonal $\{(Mo)Mo_5\}$ building blocks that are connected *via* thirty linker groups, form another class of polyoxomolybdate frameworks in which icosidodecahedral M_{30} heterometal arrays based on corner-sharing triangles can be generated.[4] The magnetism of such large molecular spin arrays, such as $(s = 5/2)_{30}$, realized as $\{Mo_{72}Fe^{III}{}_{30}\}$,[4a,5] or $(s = 1/2)_{30}$, realized as $\{Mo_{72}V^{IV}{}_{30}\}$,[4b,c] is being studied extensively as these species constitute molecular analogues of infinite frustrated spin grids such as Kagomé lattices. However, keplerates based on more than one type of magnetic heterometal linker group have thus far remained elusive. Such mixed-metal cluster compounds $\{Mo_{72}M_{30-X}M'_X\}$ are of special interest as antiferromagnetic nearest-neighbor exchange coupling between spin centers M and M′ of different spin quantum numbers $s(M) \neq s(M')$ can result in ferrimagnetic ordering with a net $S > 0$ ground state, one requirement for so-called single-molecular magnet properties based on a DS^2 anisotropy barrier between $+S_z$ and $-S_z$ states.[6] Following this rationale, we here present a useful synthetic route to a new family of ferrimagnetically ordered keplerate structures that employ different ratios of two different heterometallic linkers, V^{IV} $(s = 1/2)$ and Fe^{III} $(s = 5/2)$.

Two new compounds, $K_{23}Na_4[\{Mo^{V/VI}{}_6O_{21}(H_2O)_3(SO_4)\}_{12}(V^{IV}O(H_2O))_{15}(Mo^{V}O(H_2O))_8(Fe^{III}(H_2O)_2)_7]\cdot 150\ H_2O$ (**1**) and $K_{21}Na_2[\{Mo^{V/VI}{}_6O_{21}(H_2O)_3(SO_4)\}_{12}(V^{IV}O(H_2O))_{11}(Mo^{V}O(H_2O))_8(Fe^{III}(H_2O)_2)_{11}]\cdot 150\ H_2O$ (**2**) were obtained by addition of vanadyl sulfate and ferrous sulfate to an acidified aqueous solution of molybdate. Addition of potassium chloride results in the rapid formation of crystals (45% isolated yield) that were characterized by elemental analysis, thermogravimetry, differential scanning calorimetry, spectroscopic methods (IR, Raman, UV/VIS-NIR, ^{57}Fe Mössbauer), potentiometric titrations, magnetic measurements, and single-crystal X-ray structure analysis (including bond valence sum (BVS) calculations); this set of data was reproduced for individually synthesized batches of both compounds to rule out the formation of mixtures of variable compositions $\{Mo_{72}Mo_xFe_yV_z\}$.‡

Both quasi-isostructural spherical cluster-anions of compounds **1** and **2** have virtual icosahedral (I_h) symmetry and are composed of twelve mixed-valence $[Mo^{V}{}_nMo^{VI}{}_{6-n}O_{21}(H_2O)_3(SO_4)]^{(8+n)-}$ = $\{(Mo)Mo_5\}$ pentagonal units that are connected by 30 linker groups (Fig. 1a). Here, the linker groups comprise a "mixture" of $[Fe^{III}(OH_2)_2]^{3+}$, $[V^{IV}O(OH_2)]^{2+}$, and $[Mo^{V}O(OH_2)]^{3+}$ cations which are statistically distributed over all thirty possible linker positions. The metal centers of the linker groups, each coordinating to two terminal oxo positions of the two vicinal $\{(Mo)Mo_5\}$ units (see Fig. 1b), occupy the corners of an icosidodecahedron. Each $\{(Mo)Mo_5\}$ group consists of a central MoO_7 distorted pentagonal bipyramid (local C_{5v} symmetry) which shares its five equatorial edges with five MoO_6 octahedra. Similar to previously reported keplerate-type structures, a sulfate ligand binds to the heptacoordinate Mo center and two neighboring Mo centers in a tripodal mode (Fig. 1b). The presence of K^+ cations situated on the C_3 axes of the cluster anions just above the cluster sphere, coordinated from the outside to the six oxygen positions of the $(M–O–Mo–O–)_3$ pores, is reminiscent of the $\{Mo_{72}Mo_8V_{22}\}$[7] and $\{Mo_{72}V_{30}\}$[4b,c] structures. However, in contrast to the $\{Mo_{72}V_{30}\}$ cluster anion which contains two parallel $\{KSO_4\}_5$ rings inside the spherical shell below two sets of pentacoordinate V(IV) centers, no such arrangement and no potassium counter-cations within the water-containing cluster interior are observed in **1** and **2** as a result of the six-fold octahedral coordination of all 30 linker centers. Overall, **1** and **2** represent the first members of a new family of keplerates based on two different heterometal linker groups. Several independent techniques (elemental analysis, potentiometric titrations, and magnetic measurements) establish the following V(IV)/Fe(III)/Mo(V) (total adding to 30) ratios: 15/7/8 for **1** and 11/11/8 for **2**. Preparation of such electron-rich compounds containing an unusual icosidodecahedral array of

---

[a] *Department of Chemistry, Emory University, Atlanta, GA 30322, USA. E-mail: bbotar@emory.edu; chill@emory.edu*
[b] *Ames Laboratory, Iowa State University, Ames, IA 50011, USA. E-mail: kogerler@ameslab.gov*
[c] *Lehrstuhl für Anorganische Chemie I, Fakultät für Chemie, Universität Bielefeld, Postfach 100131, 33501, Bielefeld, Germany*
[d] *Department of Physics, Emory University, Atlanta, GA 30322, USA*

† Electronic supplementary information (ESI) available: ^{57}Fe Mössbauer, IR, Raman, UV-VIS spectra and DSC data. See DOI: 10.1039/b512244a

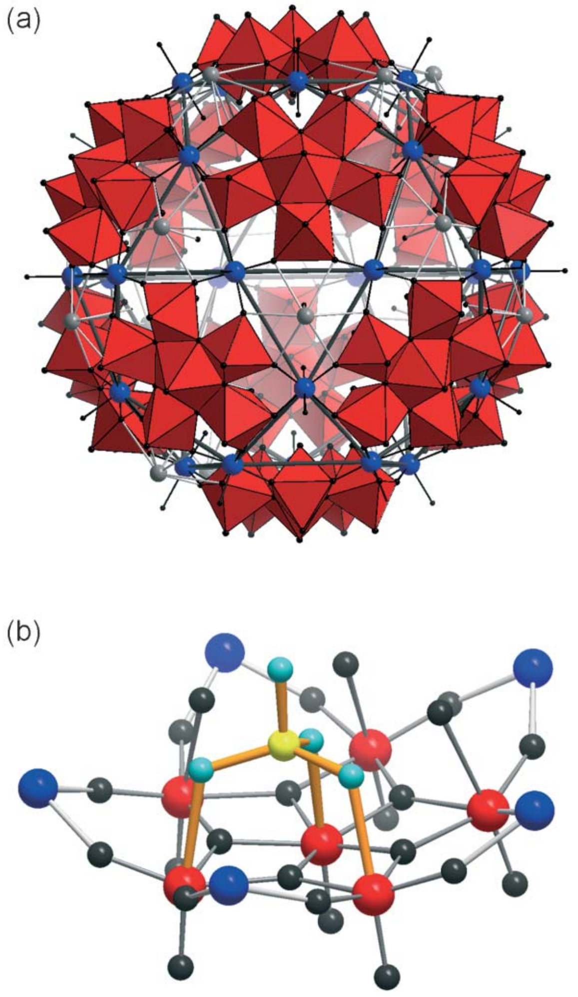

Fig. 1 (a) Schematic structure of the keplerate-type $\{Mo_{72}M_{30}\}$ cluster anions in **1** and **2** with the polyoxomolybdate $\{(Mo)Mo_5\}_{12}$ framework in polyhedral and the icosidodecahedral M_{30} linker substructure in ball-and-stick representations (Mo: red, M linker centers (V, Fe, or Mo): blue, O: black). Also emphasized are K^+ cations (light grey) coordinated to $M_3Mo_3O_6$ pores. Nearest-neighbor distances between the 30 linker centers range from 6.27 to 6.41 Å. (b) Ball-and-stick representation of a $\{(Mo)Mo_5\}M_5$ fragment. A sulfate ligand (S: yellow, orange bonds) coordinates from the inside of the cluster sphere to the $\{(Mo)Mo_5\}$ group in a tripodal mode. In the X-ray structures of both **1** and **2** the sulfate is found to be disordered over the five possible positions in which it coordinates to the central and two vicinal Mo centers of the pentagons.

three different paramagnetic metal cations is primarily achieved by using ferrous sulfate as a reducing agent. This facilitates the reduction of Mo(VI) centers, rendering the $\{(Mo)Mo_5\}$ pentagonal units (one fundamental building block of giant polyoxomolybdate structures[2c]) more reactive toward electrophiles. Subsequently, Fe(II) is oxidized to Fe(III) by O_2 (air) and then incorporated into the nucleophilic polyoxomolybdate matrix. The ^{57}Fe Mössbauer spectra of both **1** and **2** (Figure S1 in the ESI†) are consistent with the virtual absence of any Fe(II) centers and are indicative of Fe(III) centers in a slightly distorted octahedral $FeO_4(H_2O)_2$ coordination sphere. Both direct (cerimetric) and back redox titrations (see ESI), in agreement with elemental analysis results for K and Na, establish that in both **1** and **2** an additional six Mo(4d) electrons are present which are delocalized over the twelve pentagonal units. A similar type of electron delocalization has been observed for the $\{Mo_{102}\}$-type keplerate.[8]

The UV-VIS spectra of **1** and **2** also confirm the presence of Mo(V) centers: the broad absorption band extending beyond 1000 nm is clearly the result of homonuclear IVCT (intervalence charge transfer transitions) of the $Mo^V \rightarrow Mo^{VI}$ type. In accordance with the optical electronegativity difference between the atoms involved, the heteronuclear charge transfer bands (of the $V^{IV} \rightarrow Mo^{VI}$ type) are observed at much higher energy (Figure S4 in the ESI†).[9]

The magnetic properties of both **1** and **2** are dominated by ferrimagnetic ordering due to antiferromagnetic nearest-neighbor exchange interactions between $s = 1/2$ vanadyl and $s = 5/2$ iron(III) groups, observed as field-dependent maxima in the temperature-dependence of χT (Fig. 2). The even-numbered Mo(4d) electrons are strongly coupled in both compounds and do not significantly contribute to the magnetization within the experimental temperature range (2–290 K), a common property for partially reduced polyoxomolybdates.[7,8] At room temperature, the observed values for χT correspond to the sums of spin-only contributions of the heterometal spin centers: χT(290 K, **1**) = 36.3 emu K mol^{-1} compared to 36.44 emu K mol^{-1} for 15 VO^{2+} and 7 Fe^{3+} and χT(290 K, **2**) = 51.6 emu K mol^{-1} compared to 52.17 emu K mol^{-1} for 11 VO^{2+} and 11 Fe^{3+} (assuming $g = 1.98$ for VO^{2+} and $g = 2.0$ for Fe^{3+}). These values remain virtually constant with decreasing temperature down to 50 K and then increase to reach maxima at 4.5 K (**1**) and 5.5 K (**2**) that correspond to (hypothetical) $S = 9$ (**1**) and $S = 11$ (**2**) total spin states. For fields greater than 0.1 Tesla the χT maxima are quenched and shift to higher temperatures (Fig. 2), while fields smaller than 0.1 Tesla do not result in further increases of the χT maxima. Correspondingly, magnetization measurements at 2 K (insets in Fig. 2) indicate magnetic saturation with higher fields but strongly deviate from Brillouin-type behavior, indicating that low-lying excited magnetic states are still populated to a significant degree at that temperature. Given the statistic disorder of the heterometal linker centers, the magnetic properties of **1** and **2** cannot be rationalized within the framework of a single Heisenberg model, limited to a single connectivity situation, but they will need to be expressed as an average of an ensemble of all possible spin center permutations. High-field magnetization and EPR experiments will be required to elucidate the exact nature of magnetic ordering and the ground state configurations of these systems.

We have demonstrated that by a simple modification of the reaction conditions, achieved by primarily controlling the different reagent stoichiometries and reaction times, step-wise tuning of the electronic and magnetic properties of spherical keplerate-like clusters becomes a reality. We are currently exploring functionalization with different spin centers in various ratios to extend this type of cluster chemistry.

The present research is supported by NSF (grant CHE-0236686 to CLH). Ames Laboratory is operated for the U.S. Department of Energy by Iowa State University under Contract No. W-7405-Eng-82. We thank Professor B. H. Huynh for the ^{57}Fe Mössbauer data.

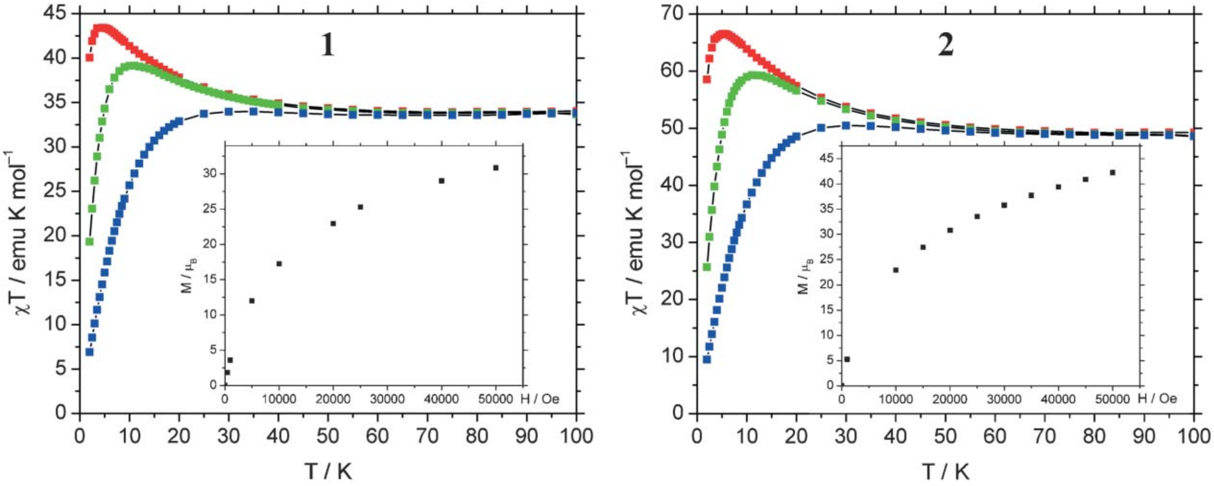

Fig. 2 Magnetic susceptibility data for compounds **1** and **2**. The temperature dependence of χT (corrected for diamagnetic and TIP contributions) within 2–100 K is shown for three fields (0.1 Tesla: red, 1.0 Tesla: green, 5.0 Tesla: blue data points), emphasizing the characteristic, field-dependent maxima. The insets show magnetization *vs.* field data recorded at 2.0 K, neither data set can be fitted to a Brillouin function.

Notes and references

‡ **1**: A solution of $Na_2MoO_4\cdot 2H_2O$ (6 g, 24.8 mmol) dissolved in 55 mL of H_2O at room temperature was acidified to pH 1.8–1.9 with H_2SO_4 (2 M; 12 mL) and then treated with 2 g of $VOSO_4\cdot 5H_2O$ (2 g, 7.9 mmol). As soon as the solution became clear, $FeSO_4\cdot 7H_2O$ (4 g, 14.4 mmol) was added and the resulting dark-blue mixture was stirred at room temperature for 3 hours. Addition of KCl (2.4 g, 32.2 mmol) dissolved in 10 mL of H_2O yielded black-violet pyramidal crystals within a few minutes. Yield 2.7 g (45% based on Mo). Anal. calcd. for $H_{446}O_{546}K_{23}Na_4S_{12}V_{15}Fe_7Mo_{80}$: K: 4.64, Na: 0.47, V: 3.94, Fe: 2.02. Found: K: 4.44, Na: 0.42, V: 3.77, Fe: 2.28%. IR (2% KBr pellet; 2000–400 cm^{-1}): 1620 (m, δ(H_2O)), 1206 (w), 1117 (w), 1052 (w) (all $\nu_{as}(SO_4)$), 963 (m-s, $\nu(Mo–O_t)/\nu(V–O_t)$), 779 (vs), 687(s), 627 (s), 567(vs), 445 (m). Resonance-Raman (in H_2O, λ_e = 1064 nm): 870(sh), 832(s), 642(m), 571(w), 456(m). VIS-NIR (in H_2SO_4/H_2O, pH = 2.0) [λ_{max}/nm (ε/L mol^{-1} cm^{-1})]: *ca.* 1100 (br), 850 (br) (both $Mo^V \rightarrow Mo^{VI}$ IVCT), 554 ($V^{IV} \rightarrow Mo^{VI}$ IVCT, $4.8\cdot 10^4$). ^{57}Fe Mössbauer: (155 K, δ = 0.50 mm/s, ΔE_Q = 0.75 mm/s and Γ = 0.45 mm/s). Cerimetric redox titrations ($\pm 1.5\ e^-$): 14.3 V(IV), 13.6 Mo(V). **2**: The synthesis of **2** is similar to that of **1** except that 1.5 g (5.9 mmol) of $VOSO_4\cdot 5H_2O$ and 9 g (32.4 mmol) $FeSO_4\cdot 7H_2O$ were used and the reaction time was extended to 16 hours. Yield 2.6 g (45% based on Mo). Anal. calcd. for $H_{454}O_{546}K_{21}Na_2S_{12}V_{11}Fe_{11}Mo_{80}$: K, 4.26, Na, 0.24, V, 2.91, Fe, 3.19. Found: K, 4.26, Na, 0.36, V, 3.09, Fe, 3.30%. IR (2% KBr pellet; 2000–400 cm^{-1}): 1621 (m, δ(H_2O)), 1205 (w), 1119 (w), 1051 (w) (all $\nu_{as}(SO_4)$), 962 (m-s, $\nu(Mo–O_t)/\nu(V–O_t)$), 777 (vs), 687(s), 627 (s), 565(vs), 446 (m). Resonance-Raman (in H_2O, λ_e = 1064 nm): 870(sh), 832(s), 642(m), 571(w), 456(m). VIS-NIR (in H_2O) [λ_{max}/nm (ε/L mol^{-1} cm^{-1})]: *ca.* 1100 (br), 840 (br) (both, $Mo^V \rightarrow Mo^{VI}$ IVCT), 548 ($V^{IV} \rightarrow Mo^{VI}$ IVCT, $5.4\cdot 10^4$). ^{57}Fe Mössbauer: (145 K, δ = 0.50 mm/s, ΔE_Q = 0.75 mm/s and Γ = 0.41 mm/s). Cerimetric redox titrations ($\pm 1.5\ e^-$): 11.7 V(IV), 13.3 Mo(V). Crystal data for **1**: $H_{446}O_{546}K_{23}Na_4S_{12}V_{15}Fe_7Mo_{80}$, M = 19391.80 g mol^{-1}, tetragonal, space group $P4_2/ncm$, a = 39.1557(12), c = 33.086(2) Å, V = 50726(4), Z = 4, ρ = 2.54 g/cm^3, μ = 2.73 mm^{-1}, F (000) = 37496, crystal size: 0.24 × 0.18 × 0.12 mm^3. A total of 452808 reflections (1.43 < Θ < 26.37°) were collected of which 26501 reflections were unique (R(int) = 0.0621). R = 0.0662 for 21697 reflections with $I > 2\sigma(I)$, R = 0.0845 for all reflections; max./min. residual electron density 3.93 (0.86 Å from V1) and −2.54 e $Å^{-3}$. Crystal data for **2**: $H_{454}O_{546}K_{21}Na_2S_{12}V_{11}Fe_{11}Mo_{80}$, M = 19295.32 g mol^{-1}, tetragonal, space group $P4_2/ncm$, a = 39.1698(14), c = 33.109(2) Å, V = 50799(4), Z = 4, ρ = 2.52 g/cm^3, μ = 2.75 mm^{-1}, F (000) = 37336, crystal size: 0.24 × 0.17 × 0.10 mm^3. A total of 558442 reflections (1.43 < Θ < 26.73°) were collected of which 27548 reflections were unique (R(int) = 0.0770). R = 0.0739 for 23847 reflections with $I > 2\sigma(I)$, R = 0.0851 for all reflections; max./min. residual electron density: 3.71 (0.87 Å from V1) and −2.69 e $Å^{-3}$. CCDC 283228 & 283229. For crystallographic data in CIF or other electronic format see DOI: 10.1039/b512244a Crystals of **1** and **2** were taken directly from the mother liquor, mounted on a cryoloop and immediately cooled to 173(2) K on a Bruker D8 SMART APEX CCD sealed tube diffractometer with graphite monochromated Mo-Kα (0.71073 Å) radiation. For both structures empirical absorption corrections using equivalent reflections were performed with the program SADABS V2.10. Structure solution, refinement and generation of publication materials were performed by using SHELXTL, V6.12 software (see ESI). Magnetic susceptibility measurements were performed using a Quantum Design MPMS-5 SQUID magnetometer in fields from 0.1 to 5.0 Tesla. All susceptibility values were corrected for inherent diamagnetism and temperature-independent paramagnetism (TIP) contributions, $\chi_{dia/TIP}(\mathbf{1})$ = -3320×10^{-6} emu mol^{-1} and $\chi_{dia/TIP}(\mathbf{2})$ = -3290×10^{-6} emu mol^{-1}.These values were derived from a combination of tabulated increments and experimentally determined susceptibilities of partially reduced diamagnetic polyoxomolybdates containing the $\{(Mo)Mo_5\}$-type fragments (to account for TIP). Dipole–dipole interactions between neighboring cluster anions in the crystal lattices of **1** and **2** are negligible due to their large separation (minimum inter-cluster V–V distance: 6.025(2) Å).

1 (*a*) P. J. Low, *Dalton Trans.*, 2005, **17**, 2821; (*b*) D. Gatteschi and R. Sessoli, *J. Magn. Magn. Mater.*, 2004, **272–276**, 1030.

2 (*a*) A. Müller, F. Peters, M. T. Pope and D. Gatteschi, *Chem. Rev.*, 1998, **98**, 239; (*b*) A. Müller, P. Kögerler and A. W. M. Dress, *Coord. Chem. Rev.*, 2001, **222**, 193; (*c*) A. Müller, P. Kögerler and C. Kuhlmann, *Chem. Commun.*, 1999, 1347.

3 (*a*) D. Gatteschi, R. Sessoli, W. Plass, A. Müller, E. Krickemeyer, J. Meyer, D. Sölter and P. Adler, *Inorg. Chem.*, 1996, **35**, 1926; (*b*) A. Müller, W. Plass, E. Krickemeyer, R. Sessoli, D. Gatteschi, J. Meyer, H. Bögge, M. Kröckel and A. X. Trautwein, *Inorg. Chim. Acta*, 1998, **271**, 9; (*c*) P. Kögerler and A. Müller, *J. Appl. Phys.*, 2003, **93**, 7101.

4 (*a*) A. Müller, S. Sarkar, S. Q. N. Shah, H. Bögge, M. Schmidtmann, Sh. Sarkar, P. Kögerler, B. Hauptfleisch, A. X. Trautwein and V. Schünemann, *Angew. Chem., Int. Ed.*, 1999, **38**, 3238; (*b*) B. Botar, P. Kögerler and C. L. Hill, *Chem. Commun.*, 2005, 3138; (*c*) A. Müller, A. M. Todea, J. Slageren, M. Dressel, H. Bögge, M. Schmidtmann, M. Luban, L. Engelhardt and M. Rusu, *Angew. Chem., Int. Ed.*, 2005, **44**, 3857.

5 A. Müller, M. Luban, C. Schröder, R. Modler, P. Kögerler, M. Axenovich, J. Schnack, P. Canfield, S. Bud'ko and N. Harrison, *ChemPhysChem*, 2001, **2**, 517.

6 D. Gatteschi and R. Sessoli, *Angew. Chem., Int. Ed.*, 2003, **42**, 268.

7 A. Müller, B. Botar, H. Bögge, P. Kögerler and A. Berkle, *Chem. Commun.*, 2002, 2944.

8 A. Müller, S. Q. N. Shah, H. Bögge, M. Schmidtmann, P. Kögerler, B. Hauptfleisch, S. Leiding and K. Wittler, *Angew. Chem., Int. Ed.*, 2000, **39**, 1614.

9 (*a*) H. So and M. T. Pope, *Inorg. Chem.*, 1972, **11**, 1441; (*b*) J. J. Altenau, M. T. Pope, R. A. Prados and H. So, *Inorg. Chem.*, 1975, **14**, 417.